

Routing Design for Pipe System Considering Natural Frequency

Jiang Fan ^{1,2,3,*} , Hongbin Xu ¹, Qingze Meng ¹ and Yumin Su ¹

¹ School of Energy and Power Engineering, Beihang University, Beijing 100191, China; sym_aero4@buaa.edu.cn (Y.S.)

² Beijing Key Laboratory of Aero-Engine Structure and Strength, Beijing 100191, China

³ Collaborative Innovation Center of Advanced Aero-Engine, Beijing 100191, China

* Correspondence: fanjiang@buaa.edu.cn

Abstract: This paper proposes a novel path planning method that considers the natural frequencies of pipes. The approach begins by presenting an adaptive decomposition method to accurately define the routing space for aero engines. Compared with the traditional decomposition method, obstacle identification efficiency is improved by more than 50%. This paper improves the initial population of the genetic algorithm based on the rapidly exploring random tree. Subsequently, a numerical surrogate model is developed to predict the natural frequencies of pipes. An evaluation function is created incorporating the weighted values of the natural frequency and the tube length. Additionally, this paper introduces several new operators to mitigate the issue of illegal paths during algorithm iterations. Finally, the proposed algorithm is demonstrated through experiments on two well-designed examples and an application in an aero engine.

Keywords: path planning; natural frequency; aero engine; genetic algorithm; rapidly exploring random tree

1. Introduction

Pipe design is among the most difficult, time-consuming tasks in the aerospace and ship industries [1–3]. Designers primarily focus on the geometric design of pipelines and often struggle to allocate sufficient time and expertise to considering the natural frequency. Applying the natural frequency calculation algorithm to the pipe's routing algorithm poses challenges. The main difficulty is that the routing algorithm does not know the final model during the process. Pipes requiring natural frequency evaluation are numerous with iterations. This problem complicates the integration of natural frequency considerations into established pipe routing methods.

This paper proposes a novel path planning method that combines the genetic algorithm (GA) and the rapidly exploring random tree [4] (RRT) while considering the natural frequency for pipe routing. The approach begins by presenting an adaptive decomposition method to accurately define the routing space for aero engines. Then, this paper improves the initial population of the genetic algorithm based on the rapidly exploring random tree. Next, this paper establishes a numerical surrogate model for the natural frequency of the pipe. It introduces an evaluation function that incorporates the weighted values of the natural frequency and the length of the pipe. Additionally, this paper introduces several new operators to mitigate the issue of illegal initial paths during algorithm iterations. Finally, the correctness of the proposed algorithm is demonstrated by the experiments on two well-designed examples and an actual aero engine.

The article is arranged as follows: Section 2 is related to works and the challenges when applying existing pipe routing algorithms to aero engines. Section 3 aims to model the routing space. Considering the numerous obstacles in actual engine models, this paper proposes an adaptive space decomposition method in Section 3. Section 4 provides a detailed introduction to the proposed method in this article. Several new genetic algorithm



Citation: Fan, J.; Xu, H.; Meng, Q.; Su, Y. Routing Design for Pipe System Considering Natural Frequency. *Appl. Sci.* **2024**, *14*, 1143. <https://doi.org/10.3390/app14031143>

Academic Editor: Rosario Pecora

Received: 17 December 2023

Revised: 4 January 2024

Accepted: 23 January 2024

Published: 29 January 2024



Copyright: © 2024 by the authors. Licensee MDPI, Basel, Switzerland. This article is an open access article distributed under the terms and conditions of the Creative Commons Attribution (CC BY) license (<https://creativecommons.org/licenses/by/4.0/>).

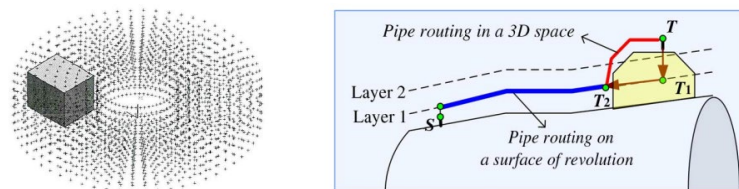
operators and a fitness function containing natural frequency are proposed. In Section 4, this paper establishes a numerical surrogate model for the natural frequency of the pipe. In the fitness function, this article normalizes the length and natural frequency to obtain the optimal path for the selected pipe. Section 5 mainly introduces a co-evolutionary algorithm for the collaborative routing of multiple pipes. In this algorithm, a new method for selecting and calculating the fitness function is constructed. Sections 6 and 7 are numerical simulation examples and conclusions to verify the algorithm proposed in this paper.

2. Related Works

Pipe routing design mainly includes two parts: ① Obstacle identification and defining the routing space and ② Pipe routing algorithms. This section will introduce the relevant research in these two parts separately.

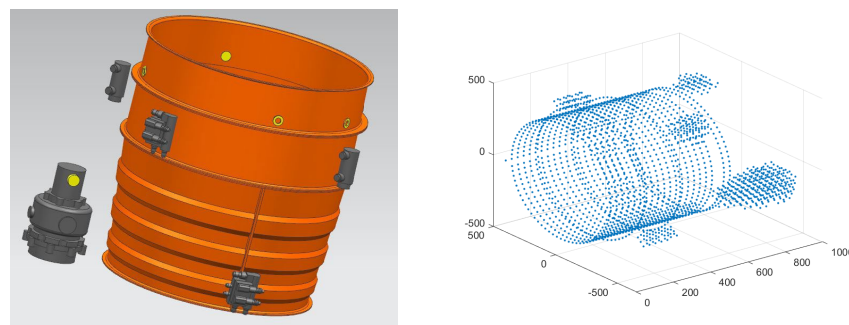
2.1. Obstacle Identification for Pipe Routing in Aero Engine

Most scholars studying pipe routing algorithms assume that the routing space is already known. This is true for some simple ship and aero-engine models. Because simple geometric models can be concatenated with a small number of containment blocks, obstacle recognition can be easily and quickly achieved. However, for geometric models with complex components, it is very difficult and time-consuming to obtain the routing space. Therefore, scholars adopt various schemes to describe the obstacle. There are primarily two types of obstacle description methods: cell decomposition (Figure 1a) and hierarchical decomposition (Figure 1b). Cell decomposition is the process of decomposing a 2D or 3D model into cells of the same size and shape. By determining the presence of obstacles in each cell, it identifies whether the pipeline can pass through. This method is widely used in traditional routing algorithms [5]. Cell decomposition demands an adequately fine grid during grid scanning to accurately depict the routing space. However, using fine-grained grids can raise concerns related to storage and computational time. For instance, the aero-engine model with the size of $400 * 600 * 800 \text{ mm}^3$ presented in Figure 2. Figure 2 is partitioned into grids based on various sizes, as depicted in Table 1.



(a) Cell decomposition (b) Hierarchical decomposition

Figure 1. Two types of decomposition method for routing space.



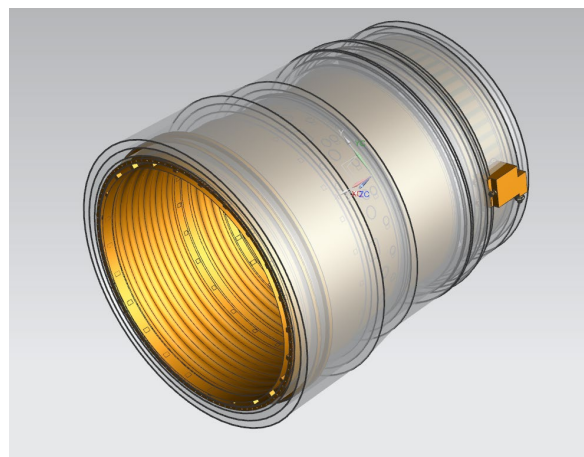
(a) Geometric model (b) Obstacle identification

Figure 2. The cell decomposition for aero engines.

Table 1. Grid size and time consumption.

Grids Size (mm)	Grids Numbers	Time (min)
16	296,298	5
12	695,196	14
8	2,360,340	50
4	19,134,375	608

Article [6] further developed the cell decomposition method, which assigns lower weights to the edges of obstacles and walls to achieve the goal of the pipeline sticking to obstacles and walls. In order to reduce the processing time during each installation of cell decomposition, article [3] proposed a hierarchical decomposition for obstacle identification. Hierarchical decomposition mainly divides the routing space into several layers along a specific direction and only identifies obstacles in the layers required for the following routing pipe (Figure 3). The hierarchical decomposition method reduces the obstacle identification time of a single pipe. However, it does not completely eliminate the need to model the entire routing space when pipes are dispersed across it. As a result, the hierarchical decomposition method has not fundamentally resolved the issue of time consumption for obstacle identification. Therefore, research into a new obstacle definition method is a prerequisite for applying pipe routing algorithms to practical aero engines.

**Figure 3.** Hierarchical decomposition. The surface represents the interface in hierarchical decomposition.

2.2. Pipe Routing Algorithms in Aero Engines

Pipe routing design has been studied for several decades, resulting in two main types of pipe routing algorithms: deterministic and heuristic algorithms [6]. Deterministic algorithms, such as the maze algorithm [7,8], the A* algorithm [9–11], and other algorithms [12–15], are extensively employed in various fields due to their fast computation time and low memory space requirements. The maze algorithm mainly simulates the behavior of waves to find paths. The maze algorithm can ensure finding the shortest path, but it requires a lot of storage space. In order to solve the problem of the maze algorithm, the A* algorithm is proposed. The A* algorithm is mainly based on greedy search algorithms, which only search for nodes closer to the endpoint, avoiding needing much storage space. Other algorithms, such as projection and graph theory, have been proposed to accelerate the search for the shortest path. The main goal of deterministic algorithms is to obtain the shortest path faster. However, it is difficult to consider constraints because the final centerline is not known during the iterations. In order to address the difficulty of considering numerous constraints in deterministic algorithms, scholars have begun to apply heuristic algorithms to pipeline routing. Typical heuristic algorithms include genetic algorithms [16–19], ant colony optimization algorithms [20–22], particle swarm algorithms [23], etc. [24,25]. These methods often rely on random behavior to obtain

paths. Genetic algorithms were the earliest to be applied in the process of pipeline routing. Scholars have applied heuristic algorithms to consider various engineering constraints, such as branch and parallel pipelines in pipeline layout. Heuristic algorithms have been proven to effectively solve engineering constraints. However, these heuristic algorithms only consider geometric constraints, without considering vibration performance, such as natural frequency. Due to the excessive number of alternative paths provided by the heuristic algorithm during each iteration, evaluating the natural frequency for each individual is time-consuming. Therefore, considering the natural frequency during pipe design is challenging due to the theoretical limitations of existing methods.

3. Adaptive Decomposition of Routing Space

The routing space encompasses various elements such as obstacles, pipes, and accessories, each with complex shapes that are challenging to accurately describe. To simplify the representation of obstacles, some researchers have approximated them as rectangular cuboids and decomposed the routing space into uniformly sized grids. Traditional cell decomposition methods encounter difficulties when dealing with the different diameters of pipes, as commonly found in aero engines. Whenever the diameter changes, the traditional methods require routing space re-decomposition, leading to time-consuming algorithms. To overcome these challenges, this paper proposes an adaptive decomposition method for the routing space. In this section, we provide a detailed introduction to the adaptive decomposition method.

The Adaptive Decomposition of Routing Space

As depicted in Figures 4 and 5, the routing space is represented as a rectangle, while equipment and prohibited pipe areas are represented by individual rectangles or their combinations. During the decomposition process, we assume that the space has already been randomly divided based on the diameter (d_{i-1}) of the ($i-1$)-th pipe. When selecting the i -th pipe with a diameter of d_i , the routing space is re-decomposed using an integer value n , which can be expressed by the following equation:

$$n = \text{int}\left(\frac{d_i}{d_{i-1}}\right) \tag{1}$$

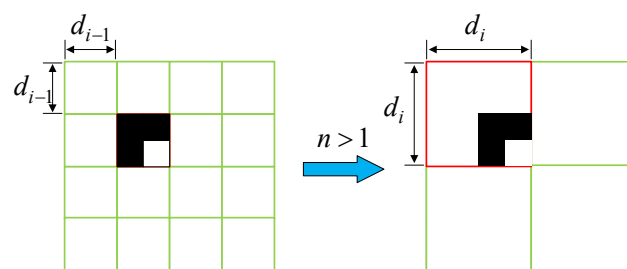


Figure 4. Adaptive decomposition ($n > 1$).

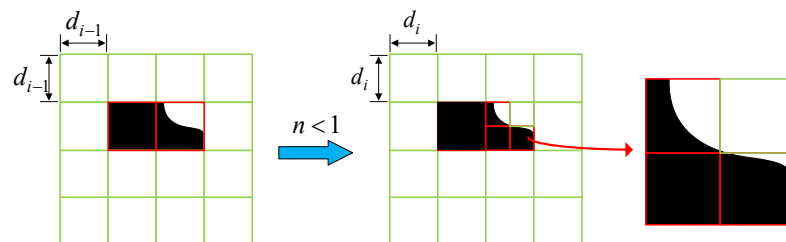


Figure 5. Adaptive decomposition ($n < 1$).

As shown in Figure 4, the adaptive grid decomposition method is illustrated. When the value of n is greater than 1, the adjacent $n * n$ grids in the original grid system are examined. If there are obstacles present within these original grids, the corresponding new grid is considered obstructed and marked with a red rectangle. Conversely, if the original grid is free from obstacles, the corresponding new grid is considered unobstructed and represented by a green rectangle. When $n < 1$ (Figure 5), the original grid will be disassembled into $n^{-1} * n^{-1}$ grids for judgment. If there are obstacles in the original grid, the new $n^{-1} * n^{-1}$ grids need to be identified. If the original grid is unobstructed, the new grid is considered unobstructed. This process helps identify and differentiate obstructed and unobstructed regions within the routing space.

By employing this method, the need to repeatedly decompose the routing space for different pipe diameters is eliminated, resulting in improved algorithm efficiency. Figure 6 demonstrates the outcomes of obstacle identification in an aero engine using the proposed adaptive decomposition algorithm. The final grid size achieved by this algorithm is 4 mm, and the entire process takes a total of 1461 s using a 2.9 GHz CPU computer. Compared with traditional cell decomposition, the efficiency of obstacle identification has been improved more than 50%.

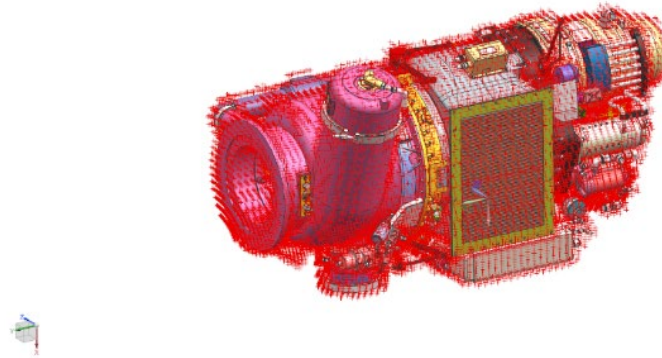


Figure 6. Routing space model by adaptive decomposition.

4. A Novel Path Planning Method for Pipe Arrangement with Considering Natural Frequency

This study aims to enhance the quality of pipe routing and ensure the pipes can withstand operational loads by considering natural frequency. Throughout the derivation of natural frequency [26], it becomes evident that calculating the natural frequency for a pipe model with a fixed geometric shape and centerline is not time-consuming. However, directly applying the natural frequency calculation algorithm to the pipe's routing algorithm poses challenges. This is because natural frequency calculation necessitates knowledge of the pipe's geometric model. In deterministic algorithms, the final centerline of the pipe is not known during the routing. Heuristic algorithms can provide the centerline and the geometric model of the pipe. During iterations, the centerline of the pipe changes. As a result, the pipe that requires natural frequency evaluation is not a single determined pipe but thousands of undetermined pipes with varying centerlines. This complexity makes it challenging to incorporate natural frequency considerations into heuristic algorithms for the existing pipe routing methods.

To overcome these challenges, this paper introduces a novel path planning method that consider the natural frequencies of pipes. To address the limitation of considering natural frequency during the iterative process, a numerical surrogate model is developed to predict pipe natural frequencies. An evaluation function is formulated, integrating weighted values of natural frequency and pipe length. Finally, the effectiveness of the proposed algorithm is demonstrated through experiments on two well-designed examples and its application in an engine.

4.1. Initial Population

The genetic algorithm is a powerful and widely applicable stochastic search optimization technique that is highly effective in solving problems that are difficult for traditional methods. Therefore, the genetic algorithm has become an effective approach for solving pipe routing problems. Previous researchers have applied genetic algorithms to single-pipe arrangements [19,27]. Some of these algorithms randomly select several spatial points to form the initial paths. However, due to the arbitrary nature of these paths, most of them intersect with obstacles or contain numerous illegal gene segments, which limits the convergence of the genetic algorithm [28]. To avoid generating a large number of illegal solutions due to random initial paths, some researchers have used deterministic algorithms such as the A* algorithm to generate initial paths and then applied random mutation or random crossover on these paths to construct the initial population.

Although these approaches reduce the number of illegal gene segments to some extent, they introduce the same gene segments in each generation due to the use of the A* algorithm, thereby reducing the global search capability of the genetic algorithm. Therefore, generating a reasonable initial population with a large number of valid gene segments becomes an effective means to address the issues of the genetic algorithm in path planning. This section utilizes the RRT algorithm to generate the initial population.

Rapidly Exploring Random Tree (RRT) Algorithm

The RRT is an incremental random sampling-based path search algorithm that can quickly find a collision-free path within the search space. In recent years, it has been widely applied in various fields and has demonstrated practicality. The RRT algorithm consists of four steps (See Figure 7). ① At the beginning, the RRT algorithm only contains the start points, some path points, and goal points. ② Secondly, computing the position of the node nearest to the random sample point. ③ Thirdly, extending a new node from the nearest node to the random sample point. ④ Fourthly, the length of the branches grown is determined by a predefined step size. RRT uses a global random sampling method to explore its directions. It ensures that the probability of expanding each node is related to the area of its Voronoi region, resulting in RRT always expanding the node in the largest surrounding empty space. This helps evenly cover the entire search space.

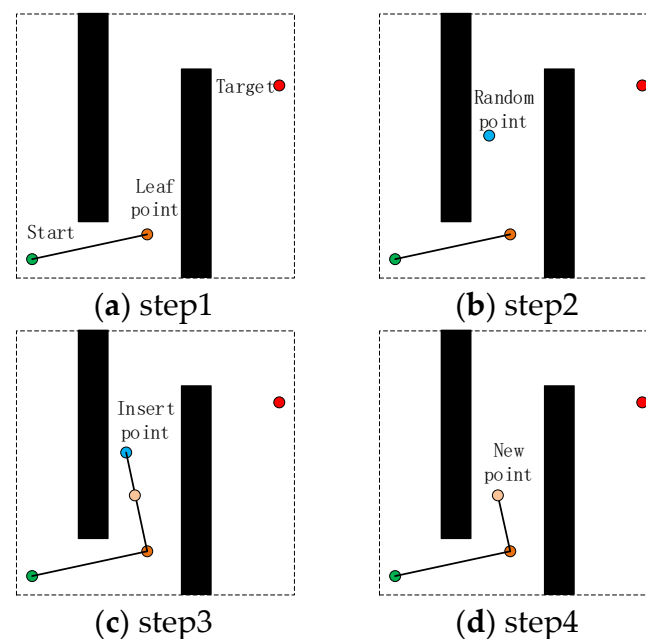


Figure 7. Rapidly Exploring Random Tree.

In this study, the RRT algorithm is utilized to generate the initial population for the genetic algorithm in the pipe routing problem. The effectiveness of the RRT algorithm is demonstrated in Figure 8, which illustrates the results of RRT with obstacles. The green and red stars represent the start and goal points, respectively, while the blue line represents the final path obtained by the RRT algorithm. Additionally, the yellow points represent the locations of supports.

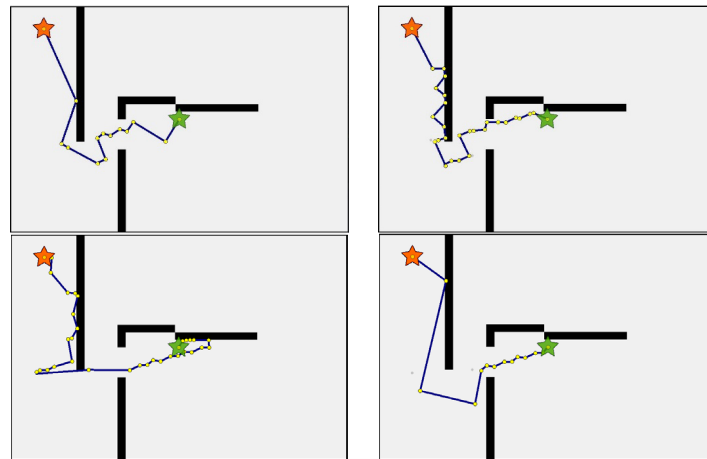


Figure 8. The initial path of a genetic algorithm based on RRT.

Although the RRT algorithm does not guarantee finding an optimal solution when obstacles are present, it exhibits randomness in pathfinding and generates paths with reasonable characteristics, such as obstacle avoidance and proximity to the shortest path. By using the RRT algorithm as the initial paths for the genetic algorithm, certain issues such as blind initialization and illegal gene segments can be addressed, leading to improved convergence speed.

To generate the initial population for the genetic algorithm, the RRT algorithm is executed multiple times (four times, listed in Figure 8) to obtain paths with the same start and goal positions. These resulting paths are discretized into spatial nodes, which form the initial population for the genetic algorithm. This approach leverages the strengths of both the RRT algorithm and the genetic algorithm to enhance the efficiency of the overall pipe routing optimization process.

4.2. Operator Design

Operator design is an important aspect of the genetic algorithm used in this study. The operators are responsible for generating new individuals in each iteration and driving the evolution of the population towards better solutions. This article proposes new crossover and mutation operators based on the RRT algorithm mentioned earlier, thereby avoiding the problem of illegal solutions during the iterative process of the algorithm.

4.2.1. Crossover Operator

The crossover operator plays a critical role in combining genetic information from two parent individuals to produce offspring with a mix of their traits. In the context of the path planning problem, crossover involves exchanging segments between two parent paths, facilitating the exploration of new paths that inherit favorable characteristics from both parents.

In this article, a single-point crossover operator is utilized. Previous studies often employed simple gene crossover strategies, resulting in many infeasible segments in the offspring individuals and the generation of numerous illegal solutions during the iterative process. To address these challenges, this article incorporates an evaluation step after a single-point crossover, as depicted in Figure 9. If the offspring contains gene points

that cannot be directly connected, the RRT algorithm is employed to generate a new path between the two gene points.

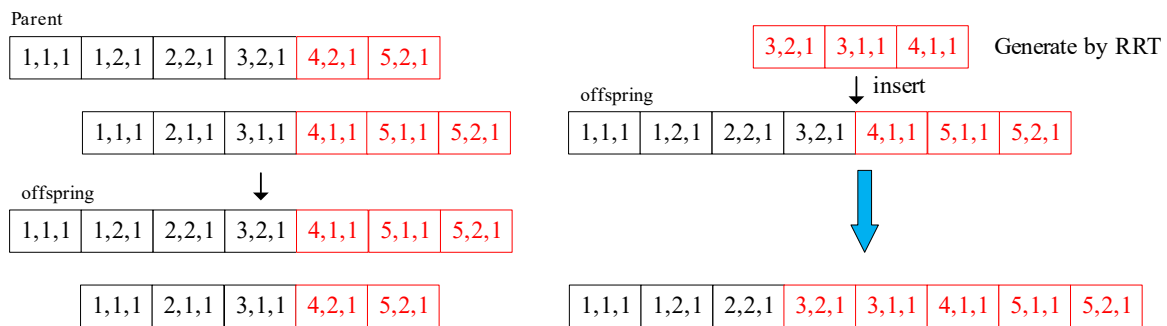


Figure 9. An example of single point cross operator. The red part represents the gene segments for cross operation.

4.2.2. Mutation Operator

The mutation operator introduces random changes to the genetic information of an individual. It helps introduce exploration in the search space and prevents premature convergence. In the case of path planning, mutation can involve modifying a portion of the path by randomly changing or shifting segments. This allows for small adjustments or the exploration of alternative paths. The four common mutation operators are used in this article. ① Add operation: on the basis of existing pipeline path individuals, randomly select two adjacent nodes and insert any point in the adjacent nodes. ② Delete operation: on the basis of existing pipeline path individuals, randomly select a point (excluding the starting and ending points) and delete a point at random. ③ Modification operation: on the basis of existing pipeline path individuals, randomly select a point (excluding the starting and ending points) and change its coordinates. ④ Interchange operation: on the basis of existing pipeline path individuals, randomly select two nodes and exchange their coordinates.

In addition to the four mutation operators mentioned above, this article proposes a new mutation operator (Figure 10). Figure 10 is a random mutation case. Figure 10 is used to demonstrate the operation process of RRT-based random mutation. We are introducing the RRT algorithm at the gene point of mutation operation, starting from the gene at the mutation site and ending at the endpoint, to find a new RRT path to insert the original gene segment. The design of these operators is crucial for the effectiveness of the genetic algorithm.

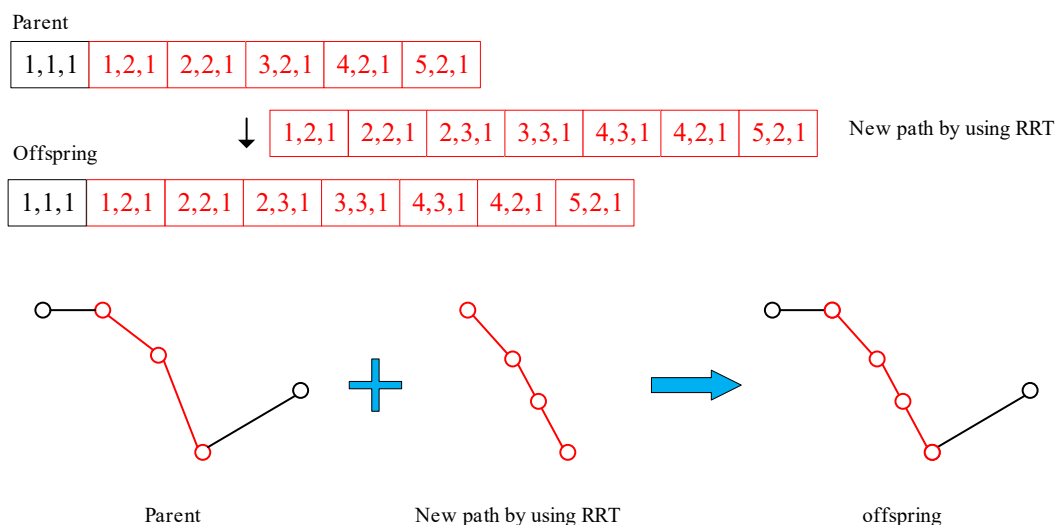


Figure 10. An example of mutation operator. The red part represents the gene segments for mutation operation.

4.3. Evaluation Function Design Considering Natural Frequency

Consider the path as composed of multiple polylines, and the intersection of the polylines is the control node of the path. Arrange the control nodes of the path in the order of connection as follows:

$$\{(x_s, y_s, z_s), \dots, (x_i, y_i, z_i), \dots, (x_t, y_t, z_t)\} \quad (2)$$

The coordinates of the starting and ending points are (x_s, y_s, z_s) and (x_t, y_t, z_t) . Constructing a suitable fitness function is essential in industries such as aircraft and ships. The primary purpose of this article is to propose a routing algorithm that considers natural frequency to solve the design problems that require the maximum natural frequency. It is necessary to minimize the pipeline's total length, maximize the natural frequency, and ensure that the spacing between adjacent supports meets the minimum distance for the installation of the pipeline and other requirements. For these pipe design problems, pipes are typically short (less than 1000 mm) but require high natural frequencies (often exceeding 10,000 Hz). Simply assigning weights to different objectives may not satisfy constraints. Therefore, this article normalizes the length and natural frequency to obtain the optimal path for the selected pipe for an evaluation function, which includes the total path length and the natural frequency of the maximum length segment, as follows:

$$\begin{aligned} \min f(\{(x_s, y_s, z_s), \dots, (x_t, y_t, z_t)\}) = & \\ \beta_1 \sum_{i=1}^m \sqrt{(x_i - x_{i-1})^2 + (y_i - y_{i-1})^2 + (z_i - z_{i-1})^2} / L_{re} & \\ + \beta_2 * F_{re} / F(L_{max}) + \beta_3 * (D_{subject} - Distance_{min}) / D_{subject} + & \\ \beta_4 * Count(N_{obstacles}) & \end{aligned} \quad (3)$$

In the proposed method, the weight values β_1 , β_2 , β_3 , and β_4 represent the relative importance of length, natural frequency, and the minimum distance between two adjacent supports. L_{max} represents the maximum length of the straight-line segment. L_{re} represents the path length when the starting and ending points are directly connected. The nature frequency of the maximum length segment is denoted as $F(L_{max})$, while F_{re} represents the natural frequency of the pipe when the starting and ending points are directly connected. The variable m represents the number of segments in the pipe path. $Count(N_{obstacles})$ is the number of nodes intersecting obstacles or other pipes. To ensure that the path can be processed, it is necessary to incorporate additional constraints based on engineering rules. One important constraint is $D_{subject}$, which limits the minimum allowable length for the pipe. D_{min} is the shortest distance between any two supports in the path. When the shortest distance is greater than $D_{subject}$, β_3 is set to 0.

A Natural Frequency Surrogate Model for Design Phase

There are several methods available to solve for the natural frequency of a pipe, such as the transfer-matrix method [29], the nonlinear vibration method [30], and the finite element method. However, these methods involve intricate numerical calculations, including mesh division and inverse matrix operations, which can be time-consuming. They become unacceptable during the iterative design process when the pipe path, shape, and support positions are not yet determined. To address the challenge of time-consuming natural frequency calculations during the iterative design process, this paper proposes a simplified approach. It treats the pipe support as a fixed constraint and introduces a surrogate model to establish a numerical replacement model for natural frequency. This surrogate model aims to expedite the calculation of the natural frequency, enabling consideration of the natural frequency and other dynamic characteristics in the pipe routing process.

The pipe for establishing a numerical surrogate model for the natural frequency is shown in Figure 11. In Figure 11, the boundary conditions are the fixed support at both ends. The reason for using fixed supports at both ends is that cantilever pipelines are not

allowed for aero engines. U is the flow velocity inside the pipe and \dot{U} is the change in flow velocity. And, respectively, T_0 represent the axial force and P_0 represents the pressure of fluid inside the pipe. x is the position coordinate along the length direction of the pipe; $p(x, t)$ represents the force. d_0 represents the outer diameter of the pipe, and h represents the thickness of the pipe. The nonlinear vibration equation of the pipeline is derived in reference [31], which is listed in Equations (4) and (5).

$$\begin{aligned} & (m_p + m_f)\ddot{u} + m_f\dot{U} + 2m_fU\dot{u} + m_fU^2u'' + m_f\dot{U}u' - \\ & EA\left(\frac{1}{2}\frac{T_0}{EA}u'' + u'' + \frac{3}{2}utu'' + \frac{1}{2}v'v''\right) - \frac{3}{2}EIv''v^{(3)} = 0 \end{aligned} \tag{4}$$

$$\begin{aligned} & (m_p + m_f)\ddot{v} + m_f\dot{U}v' + 2m_fU\dot{v} + m_fU^2v'' \\ & - \frac{1}{2}EA\left(\frac{T_0}{EA}v'' + u''v' + uv''\right) + \\ & EI\left(\left(1 + \frac{T_0}{EA}\right)v^{(4)} + \frac{3}{2}u'v^{(4)} + 3u''v^{(3)} + \frac{3}{2}u^{(3)}v''\right) = P(x, t) \end{aligned} \tag{5}$$

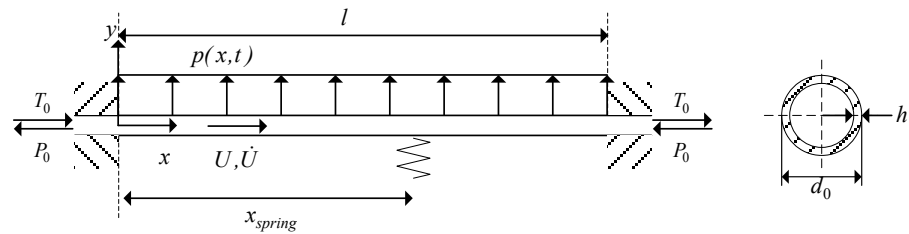


Figure 11. Calculation model of natural frequency.

In Equations (4) and (5), E is the Young’s modulus of the material, A is the cross-sectional area of the pipe, and I is the interface moment of inertia, and m_f and m_p represents the density of the liquid and the pipe material. The following dimensionless parameters are introduced.

$$\begin{aligned} \zeta &= \frac{x}{L}, \eta = \frac{u}{L}, \omega = \frac{v}{L}, \mu = UL\sqrt{\frac{m_f}{EA}} \\ \beta &= \frac{m_f}{m_f + m_p}, \tau = \frac{t}{L}\sqrt{\frac{EI}{(m_f + m_p)}} \\ \Pi_0 &= \frac{T_0L^2}{EI}, \Pi_1 = \frac{AL^2}{I}, \\ p &= \frac{PL^2}{EI} \end{aligned} \tag{6}$$

Thus, the nonlinear vibration equation of the fixed support is obtained as follows:

$$\begin{aligned} & \ddot{\eta} + \sqrt{\beta}\dot{\mu}(1 + \eta) + 2\mu\sqrt{\beta}\dot{\eta} + \mu^2\eta'' - \\ & \Pi_1\left(\frac{1}{2}\Pi_0 + 1\right)\eta'' - \Pi_1\left(\frac{3}{2}\eta'\eta'' + \frac{1}{2}\tau w''\right) - \frac{3}{2}w''w^{(3)} = 0 \end{aligned} \tag{7}$$

$$\begin{aligned} & \ddot{w} + \sqrt{\beta}\dot{\mu}w + 2\mu\sqrt{\beta}\dot{w} + \mu^2w'' - \frac{1}{2}\Pi_1\Pi_0w'' - \Pi_1(\eta''w' + \eta'w'') + \\ & (\Pi_0 + 1)w^{(4)} + \frac{3}{2}\eta'w^{(4)} + 3\eta''w^{(3)} + \frac{3}{2}\eta^{(3)}w'' = p \end{aligned} \tag{8}$$

In order to solve the above partial differential equation, the galerkin method is used to discretize the equation. Therefore, the displacement function in the pipeline can be expressed as (9) and (10)

$$\eta(\zeta, \tau) = \boldsymbol{\eta}(\zeta) * \mathbf{T}^u(\tau) = \sum \phi_r^u(\zeta) * q_r^u(\tau) \tag{9}$$

$$w(\zeta, \tau) = \mathbf{W}(\zeta) * \mathbf{T}^v(\tau) = \sum \phi_r^w(\zeta) * q_r^w(\tau) \tag{10}$$

Among them, $\eta(\zeta, t)$ and $w(\zeta, t)$ satisfies Equations (11) and (12).

$$\eta(0, \tau) = \eta(1, \tau) = \frac{\partial\eta(0, \tau)}{\partial\zeta} = \frac{\partial\eta(1, \tau)}{\partial\zeta} = 0 \tag{11}$$

$$w(0, \tau) = w(1, \tau) = \frac{\partial w(0, \tau)}{\partial \xi} = \frac{\partial w(1, \tau)}{\partial \xi} = 0 \tag{12}$$

$\phi_r(\xi)$ satisfies the following Equation (13)

$$\phi_r(\xi) = \cosh(\lambda_r \xi) - \cos(\lambda_r \xi) - \frac{\cosh(\lambda_r) - \cos(\lambda_r)}{\sinh(\lambda_r) - \sin(\lambda_r)} (\sinh(\lambda_r \xi) - \sin(\lambda_r \xi)) \tag{13}$$

λ_r satisfies the following Equation (14)

$$\cosh(\lambda_r) \cos(\lambda_r) = 1 \tag{14}$$

Multiply both sides of the equation to the left and integrate in the interval [0, 1] to obtain a discrete equation. In order to obtain the natural frequency of the pipe, the nonlinear term related to time in the equation can be ignored, so that the natural frequency can be obtained.

$$\mathbf{M}\ddot{\mathbf{T}}(\tau) + 2\mu\mathbf{G}\dot{\mathbf{T}}(\tau) + (\mathbf{K} + \mu^2\mathbf{H} + \mu\mathbf{G} + \mathbf{S})\mathbf{T}(\tau) + \mathbf{N}(\mathbf{T}(\tau)) = \mathbf{F}(\tau) \tag{15}$$

To verify the accuracy of the natural frequency calculation in this article, a curve depicting the variation in natural frequency with fluid flow velocity in the pipe is provided and compared with the results presented in article [31] (Figure 12). The material parameters are the same as in article [31], which are listed in Table 2. The curve depicting the variation in natural frequency with fluid flow velocity calculated in this article. It should be noted that natural frequencies are dimensionless in Figure 12. According to Equation (16), it can convert the dimensionless natural frequency into the actual value. $\bar{\lambda}_n$ is the dimensionless natural frequency. λ_n is the actual value of natural frequency. The relationship between natural frequency, length, and outer diameter for a steel pipe is obtained in Figure 13. In Figure 13, different colors represent the different natural frequency curves for different diameters.

$$\bar{\lambda}_n = \lambda_n L^2 \sqrt{\frac{m_p + m_f}{EI}} \tag{16}$$

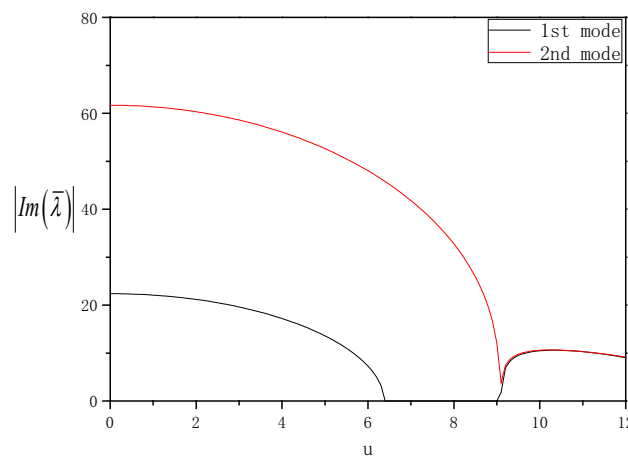


Figure 12. The natural frequency verification in this article. The curve depicting the variation in natural frequency with fluid flow velocity calculated in this article.

Table 2. The material parameters for natural frequency verification.

Name	E (Pa)	Beta	L (mm)	p	Π_0	D (mm)	H (mm)	μ
Value	1e10	0.1	2000	0	0	20	0.2	0

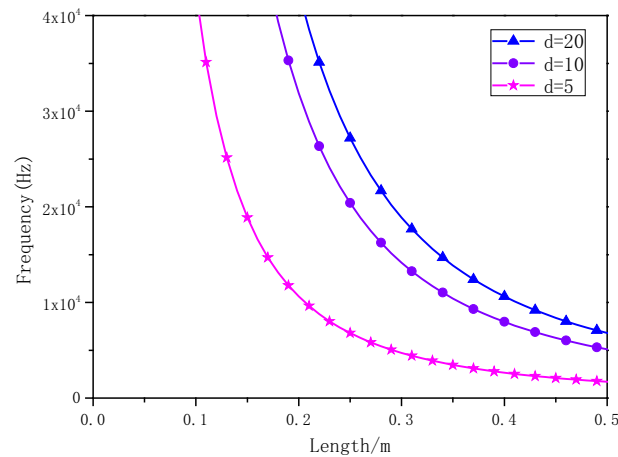


Figure 13. The natural frequency with different diameters.

Through the above derivation, it can be found that the solution of natural frequency is accompanied by a large number of inversion operations, which is very time-consuming for the path planning algorithm. Therefore, this paper uses the surrogate model [32] technology to establish the numerical model of natural frequency along with the pipe length, outer diameter, and wall thickness, so as to speed up the calculation of natural frequency. The surrogate model for natural frequency is obtained by the Equation in (17). Frequency represents the natural frequency of the pipe, A_0 , y_0 , t is the fitting constant, and L is the length of the pipe. For example, for a steel pipe with a radius of 20 mm and a wall thickness of 0.2 mm, A_0 , y_0 , and t are 7.08×10^4 , 1.08×10^2 and 4.03×10^2 (Table 3). Finally, a fast surrogate model for natural frequency has been obtained.

$$\text{Frequency} = A_0 \exp(-L/t) + y_0 \quad (17)$$

Table 3. The fitting constant parameters for different diameters.

Diameter	A_0	t	y_0
5 mm	1.44×10^7	8.01	5.4×10^3
10 mm	7.02×10^6	18.1	8.28×10^3
20 mm	7.08×10^4	1.08×10^2	4.03×10^2

5. Path Planning for Multi-Pipe System by Using Novel Collaborative Evolution

Previous studies on path planning have primarily focused on optimizing individual pipes, which may not guarantee a global optimal solution for the entire pipe system. To address this limitation and achieve an optimal solution for the entire system, this paper proposes a co-evolutionary approach for pipe routing. In this approach, each pipe in the system generates its own population, resulting in a multi-population system. By promoting cooperation and competition among the pipes, a global optimal solution is established. In the collaborative evolutionary computation of pipes, each pipe population is composed of individuals representing various paths. Heuristic algorithms like genetic algorithms are utilized to drive the evolutionary process for each pipe. During the evaluation of individuals, the evaluation process considers both coordination between different pipes and the natural frequency. This approach assigns lower fitness to individuals that positively impact coordination. Conversely, individuals that hinder coordination are assigned higher fitness. By incorporating coordination, the evolutionary process encourages the development of pipe paths that promote mutual coordination and overall system performance.

Previous works have used multi-ant colony collaborative evolutionary algorithms to solve multi-pipe routing and branch pipe routing problems [5]. However, these approaches heavily rely on the control parameters of the ant colony optimization algorithm. Another

pioneering work [27] was the first to utilize genetic algorithm co-evolution to address multi-pipe routing problems. Nevertheless, these methods lacked consideration for engineering constraints and the natural frequency of pipes. Moreover, they solely assessed the coordination relationship between optimal individuals from different populations, without achieving true co-evolution.

To overcome these limitations, this paper proposes a novel collaborative evolution method (See Figure 14). In Figure 14, the distinctive aspect of this method is highlighted in red, which sets it apart from other collaborative evolutionary algorithms. The approach involves N populations, each containing m initial paths obtained through the RRT algorithm. After acquiring the initial fitness values of each individual, the evolution proceeds sequentially based on the order of the initial populations. During population evolution, a path is randomly selected from each population, forming the temporary solution for the current system. The fitness value of this temporary solution is evaluated using Equation (3). This process is repeated k times to obtain the average fitness value and update the fitness values of each individual. The above evolutionary process continues until the maximum number of generations is reached.

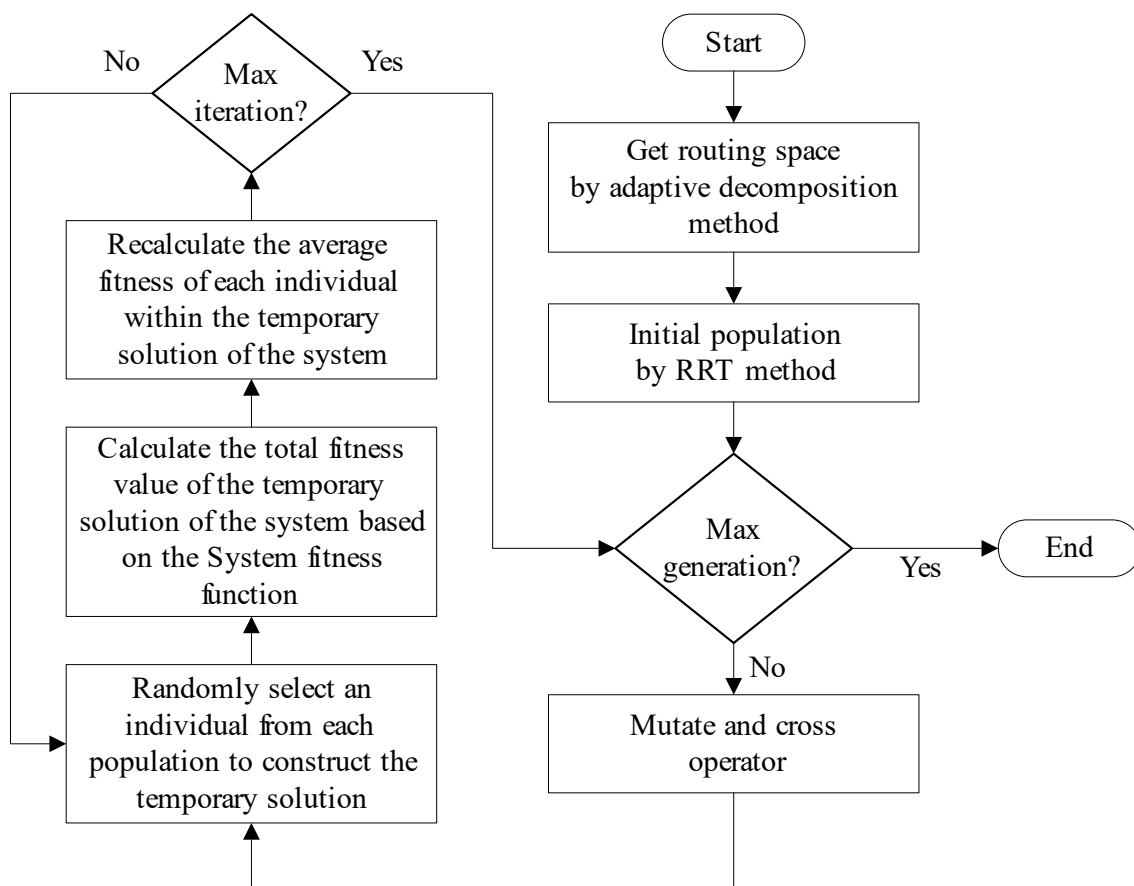


Figure 14. Path planning for multi-pipe system by using novel collaborative evolution.

Figure 15 is the detailed diagram of two pipes in the red part of Figure 14. Figure 15 is a pipe system with two pipes. The population number of each pipeline is 4. First, record its current fitness function and the number of times selected. Then, randomly select a path from each population and repeat it for k times (k = 3 in Figure 15) to form a temporary solution of the pipe, evaluate the temporary solution of the system according to Equation (3) (such as k1 in Figure 15), obtain the average fitness value of the pipe, and start the next update.

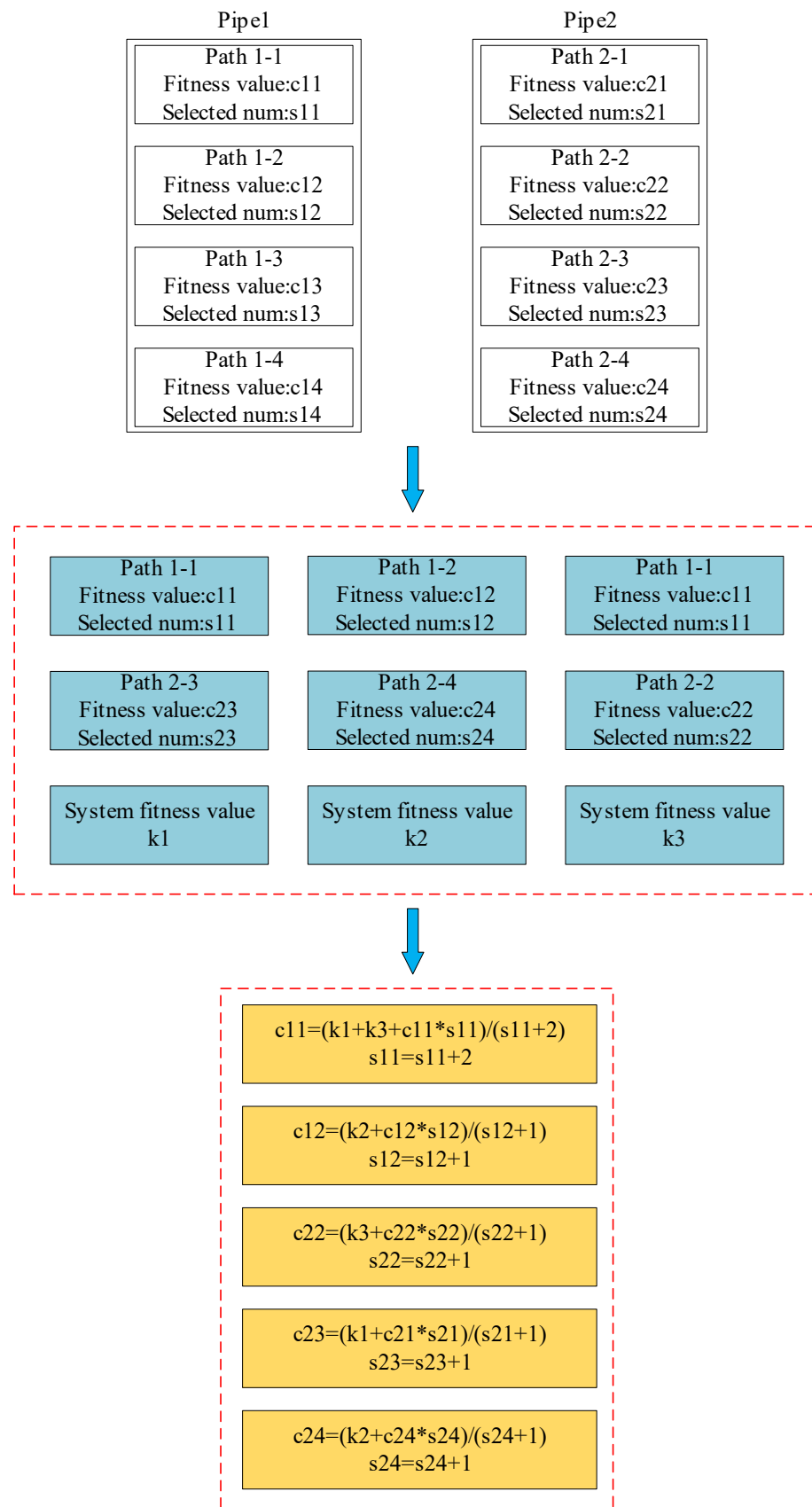


Figure 15. The detailed diagram of two pipes in the red part of Figure 14.

6. Simulations and Results

Three experiments were carried out to demonstrate the feasibility and effectiveness of the proposed algorithms. The first and second cases were based on a well-designed pipe routing problem in a 2D plane, and it was used to verify the optimization performance of the algorithms, for instance, the path searching ability, the convergence rate and speed, as well as the robustness. The third experiment involved applying the proposed algorithms to an aero-engine model with a complex and narrow routing space. This case aimed to demonstrate the practicality and effectiveness of the algorithms in handling real-world engineering scenarios with numerous obstacles and constraints. The optimization performance was evaluated in terms of the ability to find optimal or near-optimal pipe paths that consider the natural frequency, while also meeting various engineering constraints.

6.1. Single Pipe Path Planning in Two-Dimensional Environment

A routing space is depicted in Figure 16 with several obstacles. The routing space is a rectangular area measuring $400 \times 300 \text{ mm}^2$. The obstacles are represented by black rectangles. The red and green stars indicate the starting and ending points of the pipe. The evaluation function factors are as follows: $\beta_1 = 0.5$, $\beta_2 = 0.5$, $\beta_3 = 0.5$, and $\beta_4 = 1 \times 10^6$ the minimum length requirement is set to $L_{\min} = 30$. The pipe material is 0cr18ni9 with a radius of 20 mm and a wall thickness of 0.2 mm. The natural frequency surrogate model factors are $A_0 = 7.08 \times 10^4$, $y_0 = 1.08 \times 10^2$, and $t = 4.03 \times 10^2$. The number of the initial population is 5. The blue line represents the path of pipe. Additionally, the yellow dots indicate the specific positions along its route where the pipe should be supported.

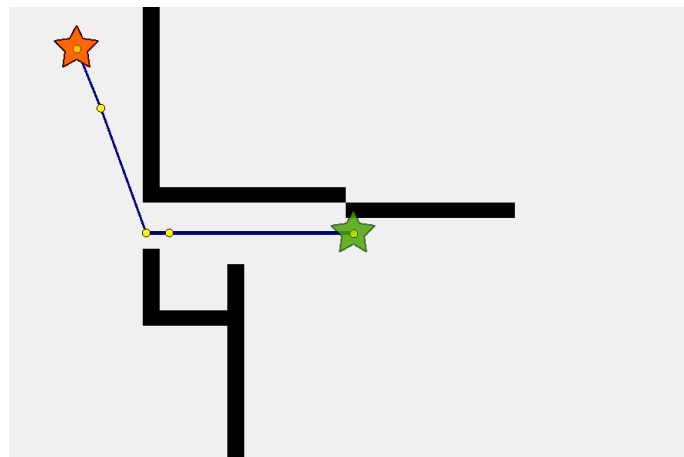
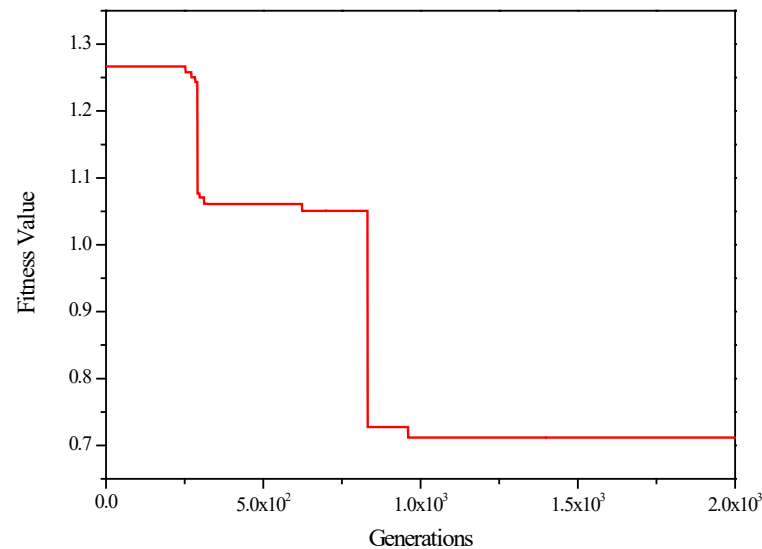


Figure 16. Simulation result in case study 1. The red and green stars indicate the starting and ending points of the pipe.

The statistical results are shown in Table 4. Figure 16 is the result of case study 1. Figure 17 displays the fitness curves of the simulations. In Figure 16, the minimum segment occurs between the second and third support points with a distance of 30 mm. Case study 1 shows the pipeline's centerline obtained by the routing algorithm, not the 2D model of the pipeline. In case study 1, the turning radius issue was not considered; only the pipeline's centerline was displayed. From Figure 16, it can be found that the proposed method can meet the requirements and ensure collision avoidance between the layout environment. This article takes into consideration the natural frequency of the longest segment and optimizes the support positions while planning the path. During the optimization process of the support positions, the distance between two support positions must meet the specified requirement, which in this case is a minimum distance of 30 mm. According to the data in Table 4, the natural frequency of the longest segment is 8079.57 Hz, the total length is 239.6 mm, the convergence value of the evaluation function is 0.71161, and the convergence is reached after 825 generations.

Table 4. Information of the piping paths in case study 1.

Case	Length (mm)	Frequency (Hz)	Minimum Segment (mm)	Fitness Value	Generations
1	239.6	8079.57	30	0.71161	825

**Figure 17.** Fitness value in case study 1.

6.2. Multi-Pipe Path Planning in Two-Dimensional Environment

After validating the correctness of routing a single pipe, further validation of the algorithm for multiple pipes was conducted. The environment and simulation results are presented in Figure 18. In this particular case of the multi-pipe routing algorithm, there are three pipes and each pipe has an initial population of 5. The parameters used in this case are the same as in case 1. The fitness value of the current optimal path is outputted every 10 generations. The fitness curves of the simulations are shown in Figure 19. At the beginning of the iteration, the evaluation function has a relatively high value due to the issue of initial paths of several pipelines crossing each other. As the iteration progresses, the phenomenon of intersecting disappears, resulting in a rapid decrease in the fitness value until convergence. The results are summarized in Table 5. In Figure 18, the red, green, and blue lines represent the centerlines of pipes P1, P2, and P3. It can be observed from Figure 18 that the multi-pipe algorithm proposed in this paper effectively achieves obstacle avoidance among multiple pipes in complex environments. By considering the natural frequency of the longest straight segment and the shortest segment in the evaluation function, the path planning result is no longer solely focused on achieving the shortest path. From Figure 18 and Table 5, it can be observed that the total path length of the red pipe is 650.2 mm, with the shortest segment length of 79.7 mm, which exceeds the set constraint of 30 mm. The natural frequency of the longest segment is 2686.6 Hz, and there are two clamp support positions. Convergence is achieved after 2520 generations. The total path length of the green pipe is 544.6 mm, with the shortest segment length being 46.7 mm. The natural frequency of the longest segment is 20,862.5 Hz, and there are five support positions. Convergence is achieved after 3510 generations. The total path length of the blue pipeline is 77.8 mm, with the shortest segment length being 43.4 mm, the natural frequency of the longest segment being 46,053.8 Hz, and having one support position. The convergence algebra is 2200 generations.

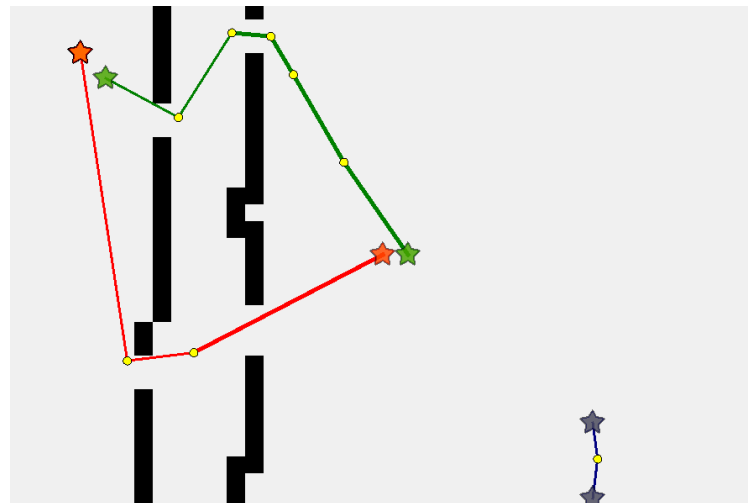


Figure 18. Simulation result in case study 2. The different stars indicate the different start and end points of the pipe.

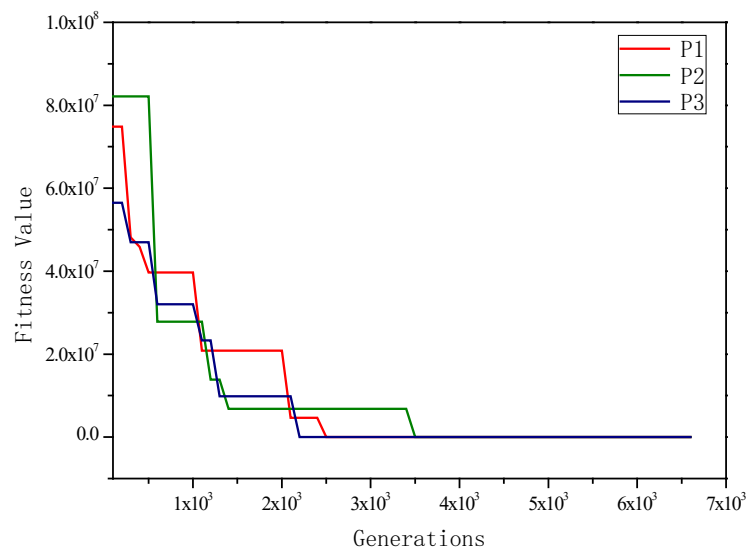


Figure 19. Fitness value in case study 2.

Table 5. Information of the paths in case study 2.

Case	Pipe	Length (mm)	Frequency (Hz)	Minimum Segment (mm)	Fitness Value	Generations
2	1	650.2	2686.6	79.7	370.4	2520
	2	544.6	20,862.5	46.7	2.50362	3510
	3	77.8	46,053.8	43.4	402.752	2200

6.3. Application

After validating the proposed method in 2D plane cases, it is demonstrated that the algorithm can effectively consider the natural frequency of the longest segment, ensuring that the routing results can withstand the actual engineering loads. In case study 3, the algorithm is applied to a real engine model. The model used in this article is the Garrett GTCp85-98D gas turbine engine, which was obtained through an open-source model acquisition method. The model is a scaled model. The routing space in this model is filled with numerous obstacles and accessories, posing challenges for pipe arrangement (Figure 20).

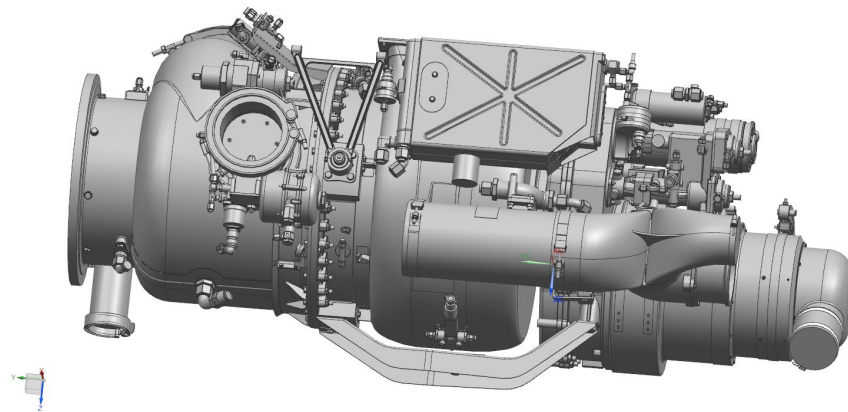


Figure 20. Aero engine in case study 3.

Using the adaptive decomposition method in this article to model the routing space. The final grid size achieved by the adaptive decomposition and the entire process takes a total of 1461 s in a 2.9GHz CPU computer. In case study 3, the number of pipes is 12, and the diameters are 5 mm, 10 mm, and 20 mm. The material is 0cr18ni9 which is commonly used in aero engines. In the surrogate model of natural frequency for the longest segment, the parameters are shown in the Table 2.

Pretreatment on the Direction Constraint of the Pipe Nozzles

The initial pipe nozzles may be covered by the obstacle extension; to eliminate the impact and meet the direction constraints on pipe nozzles, the locations of the connection points will be extended outward appropriately in advance. The grid paths between the initial nozzles and the new nozzles are straight, which should be kept and marked as obstacles. When finishing the routes between the new pipe nozzles, both kinds of paths will be connected together to obtain a complete layout. Note that the extension distance must be greater than the maximum distance of obstacle extension. In general, the same extension distance will be specified for all pipe nozzles at first; to obtain better results, the extension distances of some nozzles could be adjusted according to the feedback of the initial layouts, in this case, when the extension distance of each nozzle is set to 8 mm (Table 6).

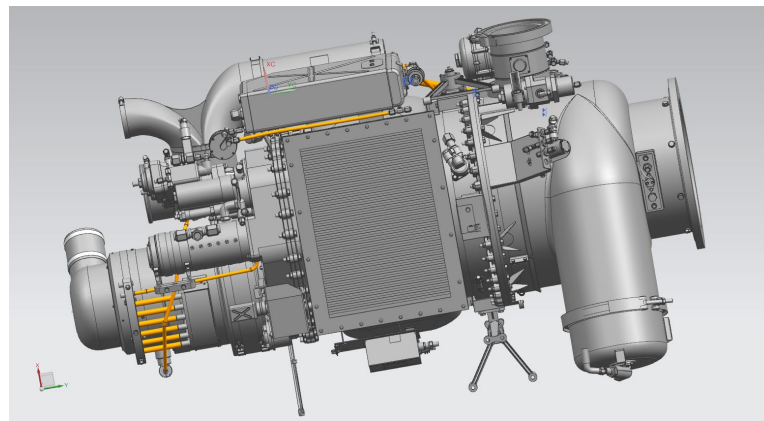
Table 6. Pretreatment of the direction constraint of the pipe nozzles in case study 3.

Case	Pipe	Diameter (mm)	Extension Distance of Each Pipe Nozzle (mm)
3	P1~P6	5	8
	P7~P11	10	
	P12	20	

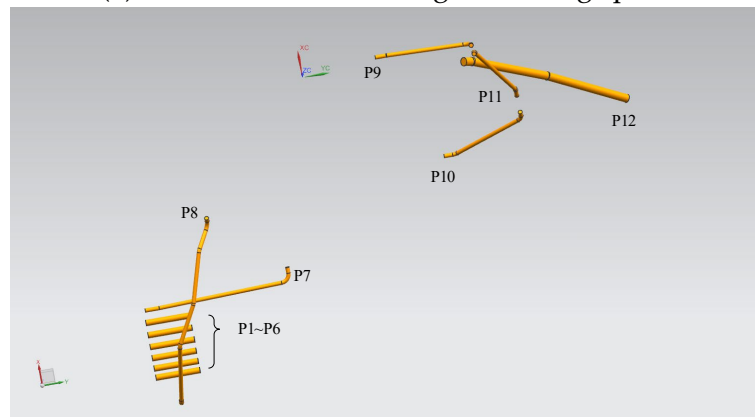
After these pretreatments, the pipes can be arranged by following steps: (a) extend the pipe nozzles outward by 8 mm; (b) search the path of the current pipe with the proposed algorithms; (c) smooth the route to allow for actual processing. In Example 3 of this article, the fillet radius of all the pipelines is 3 mm. Figure 21a shows the full view of the engine routing space. Figure 21b shows the pipe view after hiding the engine parts.

The obtained layout is shown as Figure 21. As can be seen, to avoid collisions between pipes, many bending parts are involved. In Figure 21, all turning points are the fixed positions of the clamps, thereby dividing the pipeline into multiple segments and increasing the natural frequency of the pipeline. From the values of the evaluation function in Table 7, it can be found that the fitness function designed in this article effectively normalizes the magnitude mismatch between pipe length and natural frequency, achieving the goal of considering natural frequency during the routing process. When the fitness value is 1, this

indicates that the pipeline joint is directly connected. When the fitness value is greater than 1, this indicates that the shortest segment of the pipeline falls below the required 30 mm length, and β_3 takes on a value of 0.5. Conversely, when the fitness function is less than 1, this implies that the optimization process of the pipeline has successfully increased the natural frequency by optimizing the bending positions and strategically setting clamps. It is worth noting that for pipe 12, conventional algorithms like maze, A*, and other greedy algorithms generally provide direct connection results as their main aim is to find the shortest path. However, due to the large outer diameter and considerable length of pipe 12, its natural frequency value is very small. In contrast, the proposed algorithm goes beyond simple shortest-path solutions and significantly improves the natural frequency of pipelines by iteratively optimizing pipeline path points during the layout process.



(a) The full view in the engine routing space



(b) The pipe view after hiding the engine parts.

Figure 21. The layout of 12 pipes.

Table 7. Result of the pipe paths in case study 3.

Case.	Pipe	Length (mm)	Frequency (Hz)	Minimum Segment (mm)	Fitness Value
3	P1~P6	19.1	1.3×10^6	19.1	1.18
	P7	48.3	5.30×10^3	48.3	1
	P8	70.7	2.08×10^6	10	1.19
	P9	39.8	7.97×10^3	39.8	1
	P10	33.1	1.17×10^4	33.1	1
	P11	31.1	1.33×10^4	31.1	1
	P12	67.8	1.47×10^4	33.3	0.87

Overall, the results of the experiments illustrate the robustness and efficiency of the proposed algorithms in path planning for pipelines, considering not only the shortest path but also the critical factor of natural frequency to ensure the pipelines can withstand actual engineering loads and vibrations.

7. Conclusions

In this article, a novel and effective pipe path planning method considering natural frequency has been developed. This article presents an adaptive decomposition method for modeling the narrow routing space in actual aero-engine applications. The adaptive decomposition method contributes to the accurate modeling of the narrow routing space, enabling more effective and efficient pipe design in aero-engine applications. Then, the proposed method addresses the issues of illegal initial paths by improving the initial population using RRT. Additionally, several novel operators are introduced to enhance the performance of the GA. The evaluation function considers the trade-off between natural frequency and length by applying appropriate weights. Moreover, a new co-evaluation algorithm is proposed for multi-pipe path planning, which initializes the chromosomes of each pipe using the connection points generated around the routed pipe and evolves them through the iterative process. Simulations demonstrate that the proposed algorithm effectively generates optimal layouts for different piping cases. Several conclusions are listed as follows:

- (1) This article proposes a new algorithm for the spatial modeling of aero engines and ships. This algorithm accelerates the recognition efficiency of obstacles in pipeline layout space by adaptively adjusting the grid size, merging and decomposing existing grids. Thus, existing algorithms can be applied to the spatial extraction of real engines and ships. Compared with traditional cell decomposition, the efficiency of obstacle identification has been improved by more than 50%.
- (2) This article integrates an RRT algorithm, a genetic algorithm, and other optimization algorithms to introduce novel selection, mutation, crossover, and other operators, leading to the development of a new multi-pipe routing algorithm. By formulating appropriate fitness functions, the natural frequency of the longest segment in the pipeline route is considered, ensuring that the laid pipeline meets practical requirements, such as avoiding resonance, and can be directly applied to real engineering environments. This comprehensive approach addresses the challenges of pipeline layout and optimization, enhancing the efficiency and effectiveness of the entire process.
- (3) The proposed algorithms in this article demonstrate their ability to generate connected paths between the pipe nozzles while satisfying various constraints. These constraints include maintaining the direction constraints on the nozzles, ensuring collision avoidance between pipes and the layout environment. The algorithms consider the complex routing space, obstacles, and diversity of constraints to optimize the pipe paths effectively. By incorporating techniques such as genetic algorithms, RRT, and co-evolutionary methods, the algorithm in this article can consider the maximum interval in the pipeline route, thereby reducing the maximum interval length and reducing its vibration response. This comprehensive approach contributes to the generation of optimal and feasible pipe arrangements in complex engineering scenarios, such as aero engines and other applications where precise and efficient pipe routing is crucial.

Author Contributions: Conceptualization, J.F.; methodology, writing, H.X.; validation, Q.M.; formal analysis, Q.M.; investigation, Y.S. All authors have read and agreed to the published version of the manuscript.

Funding: This study was supported by the National Science and Technology Major Project of China (J2019-I-0008-0008 and J2019-IV-0002-0069).

Institutional Review Board Statement: Not applicable.

Informed Consent Statement: Not applicable.

Data Availability Statement: The original contributions presented in the study are included in the article, further inquiries can be directed to the corresponding author.

Conflicts of Interest: The authors declare no conflicts of interest.

References

1. Qian, X.L.; Ren, T.; Wang, C.E. A Survey of Pipe Routing Design. In Proceedings of the 2008 Chinese Control and Decision Conference, Nanchang, China, 2–4 July 2008.
2. Fan, X.; Lin, Y.; Ji, Z. The ES Model for Ship Pipes Routing Design. In Proceedings of the 2010 8th World Congress on Intelligent Control and Automation (WCICA), Jinan, China, 7–9 July 2010; pp. 2787–2792.
3. Liu, Q.; Wang, C. A Graph-Based Pipe Routing Algorithm in Aero-Engine Rotational Space. *J. Intell. Manuf.* **2015**, *26*, 1077–1083. [[CrossRef](#)]
4. Jeong, I.-B.; Lee, S.-J.; Kim, J.-H. Quick-RRT*: Triangular Inequality-Based Implementation of RRT* with Improved Initial Solution and Convergence Rate. *Expert Syst. Appl.* **2019**, *123*, 82–90. [[CrossRef](#)]
5. Jiang, W.-Y.; Lin, Y. A Co-Evolutionary Improved Multi-Ant Colony Optimization for Ship Multiple and Branch Pipe Route Design. *Ocean Eng.* **2015**, *102*, 63–70. [[CrossRef](#)]
6. Dong, Z.; Bian, X. Ship Pipe Route Design Using Improved A* Algorithm and Genetic Algorithm. *IEEE Access* **2020**, *8*, 153273–153296. [[CrossRef](#)]
7. Fan, J.; Ma, M. Research on Automatic Laying of External Pipelines for Aircraft Engines. *Mach. Des.* **2003**, *20*, 21–23.
8. Lee, C.Y. An Algorithm for Path Connections and Its Applications. *IRE Trans. Electron. Comput.* **1961**, *10*, 346–365. [[CrossRef](#)]
9. Wu, H. Research on Pipeline Automatic Layout and Optimization Technology in Complex Products. Master's Thesis, Beijing Institute of Technology, Beijing, China, 2015.
10. Chen, Y.; Li, T.; Yin, M. Research on Pipeline Automatic Laying Based on Improved A* Algorithm. *J. Ordnance Equip. Eng.* **2016**, *39*, 91–95.
11. Dong, Z. *Research on Automatic Layout Method and Application of Ship Pipeline*; Dalian University of Technology: Dalian, China, 2017.
12. Hightower, D. A Solution to Line-Routing Problems on the Continuous Plane. In Proceedings of the 6th Annual Design Automation Conference, Miami Beach, FL, USA, 8–12 June 1969; Association for Computing Machinery: New York, NY, USA, 1969; Volume 6, pp. 11–34. [[CrossRef](#)]
13. Wang, C.; Liu, Q. Projection and Geodesic-Based Pipe Routing Algorithm. *IEEE Trans. Autom. Sci. Eng.* **2011**, *8*, 641–645. [[CrossRef](#)]
14. Min, J.-G.; Ruy, W.-S.; Park, C.S. Faster Pipe Auto-Routing Using Improved Jump Point Search. *Int. J. Nav. Archit. Ocean Eng.* **2020**, *12*, 596–604. [[CrossRef](#)]
15. Park, J.H.; Storch, R.L. Pipe-Routing Algorithm Development: Case Study of a Ship Engine Room Design. *Expert Syst. Appl.* **2002**, *23*, 299–309. [[CrossRef](#)]
16. Kim, D.G.; Corne, D.; Ross, P. *Industrial Plant Pipe-Route Optimization with Genetic Algorithms*; Springer: Berlin, Germany, 1996.
17. Wu, J. *Optimization of Ship Branch Pipeline Spatial Layout Based on Collaborative Evolution*; Dalian University of Technology: Dalian, China, 2008.
18. Feng, H. *Research on the Design Method of Automatic Pipeline Laying for Mechanical Equipment*; Harbin Institute of Technology: Harbin, China, 2009.
19. Ito, T. A Genetic Algorithm Approach to Piping Route Path Planning. *J. Intell. Manuf.* **1999**, *10*, 103–114. [[CrossRef](#)]
20. Wang, Y.; Yu, Y.; Li, K.; Zhao, X.; Guan, G. A Human-Computer Cooperation Improved Ant Colony Optimization for Ship Pipe Route Design. *Ocean Eng.* **2018**, *150*, 12–20. [[CrossRef](#)]
21. Fan, X.; Lin, Y.; Ji, Z. Multi Ant Colony Coevolution for Parallel Layout Optimization of Ship Multiple Pipelines. *J. Shanghai Jiaotong Univ.* **2009**, *2*, 193–197.
22. Dorigo, M.; Gambardella, L.M. Ant Colony System: A Cooperative Learning Approach to the Traveling Salesman Problem. *IEEE Trans. Evol. Comput.* **1997**, *1*, 53–66. [[CrossRef](#)]
23. Liu, Q.; Wang, C. A Discrete Particle Swarm Optimization Algorithm for Rectilinear Branch Pipe Routing. *Assem. Autom.* **2011**, *31*, 363–368. [[CrossRef](#)]
24. Liu, L.; Liu, Q. Multi-Objective Routing of Multi-Terminal Rectilinear Pipe in 3D Space by MOEA/D and RSMT. In Proceedings of the 2018 3rd IEEE International Conference on Advanced Robotics and Mechatronics (IEEE ICARM), Singapore, 18–20 July 2018; pp. 462–467.
25. Liu, Q.; Wang, C. Multi-Terminal Pipe Routing by Steiner Minimal Tree and Particle Swarm Optimisation. *Enterp. Inf. Syst.* **2012**, *6*, 315–327. [[CrossRef](#)]
26. Cigeroglu, E.; Ozguven, H.N. Nonlinear Vibration Analysis of Bladed Disks with Dry Friction Dampers. *J. Sound Vib.* **2006**, *295*, 1028–1043. [[CrossRef](#)]
27. Dong, Z.; Lin, Y. Ship Pipe Routing Method Based on Genetic Algorithm and Cooperative Coevolution. *J. Ship Prod. Des.* **2017**, *33*, 122–134. [[CrossRef](#)]

28. Liao, H.; Zhang, W.; Dong, X.; Poczos, B.; Shimada, K.; Kara, L.B. A Deep Reinforcement Learning Approach for Global Routing. *J. Mech. Des.* **2020**, *142*, 061701. [[CrossRef](#)]
29. Li, S.; Liu, G.; Kong, W. Vibration Analysis of Pipes Conveying Fluid by Transfer Matrix Method. *Nucl. Eng. Des.* **2014**, *266*, 78–88. [[CrossRef](#)]
30. Qian, Q.; Wang, L.; Ni, Q. Nonlinear Responses of a Fluid-Conveying Pipe Embedded in Nonlinear Elastic Foundations. *Acta Mech. Solida Sin.* **2008**, *21*, 170–176. [[CrossRef](#)]
31. Lee, S.I.; Chung, J. New Non-Linear Modelling for Vibration Analysis of a Straight Pipe Conveying Fluid. *J. Sound Vib.* **2002**, *254*, 313–325. [[CrossRef](#)]
32. Shan, S.; Wang, G.G. Survey of Modeling and Optimization Strategies to Solve High-Dimensional Design Problems with Computationally-Expensive Black-Box Functions. *Struct. Multidiscip. Optim.* **2010**, *41*, 219–241. [[CrossRef](#)]

Disclaimer/Publisher’s Note: The statements, opinions and data contained in all publications are solely those of the individual author(s) and contributor(s) and not of MDPI and/or the editor(s). MDPI and/or the editor(s) disclaim responsibility for any injury to people or property resulting from any ideas, methods, instructions or products referred to in the content.